

**Photoinduced Intramolecular Charge Transfer in Donor-Acceptor  
Biaryls and Resulting Applicational Aspects  
Regarding Fluorescent Probes and Solar Energy Conversion**

by

**Michael Maus**

ISBN: 1-58112-030-3

**DISSERTATION.COM**



1998

Copyright © 1998 Michael Maus

All rights reserved.

ISBN: 1-58112-030-3

Dissertation.com

1998

**Photoinduced Intramolecular Charge Transfer in Donor-Acceptor Biaryls and  
Resulting Applicational Aspects  
Regarding Fluorescent Probes and Solar Energy Conversion**

D i s s e r t a t i o n  
zur Erlangung des akademischen Grades  
d o c t o r r e r u m n a t u r a l i u m  
(Dr. rer. nat.)  
im Fach Chemie  
eingereicht an der

Mathematisch-Naturwissenschaftlichen Fakultät I  
der Humboldt-Universität zu Berlin  
von

Diplom-Chemiker Michael Maus  
geboren am 29.09.1966 in Köln

Präsident der Humboldt-Universität zu Berlin  
Prof. Dr. H. Meyer

Dekan der Mathematisch-Naturwissenschaftlichen Fakultät I  
Prof. Dr. J. Rabe

Gutachter: 1. Prof. Dr. W. Rettig  
2. Dozent Dr. R. Lapouyade  
3. Dozent Dr. J. Bendig

Tag der mündlichen Prüfung: 02. Juli 1998

## Danksagungen

In erster Linie bedanke ich mich bei meinem Doktorvater Herrn Prof. W. Rettig, der mir die Arbeit erst ermöglichte und mich durch viele interessante Diskussionen unterstützte. Außerdem danke ich Ihm dafür, daß er mir den Besuch zahlreicher Tagungen erlaubte.

Natürlich gilt mein Dank entsprechend Dr. R. Lapouyade, der als langjähriger „Weggefährte“ von Prof. Rettig, die Idee das DMABN durch einen Benzolring zu erweitern mitausbrütete und die Donor-Akzeptor Biphenyle schließlich zur Verfügung stellte. Außerdem bedanke ich mich bei ihm, daß er die Funktion als Gutachter übernommen hat.

Herrn Dr. Bendig danke ich sehr dafür, daß er sich trotz des enormen Zeitdrucks bereit erklärt hat, meine Arbeit zu begutachten.

Der gesamten Arbeitsgruppe danke ich für das tolle Arbeitsklima und viele anregende, hilfreiche Diskussionen.

Sehr wichtige und teilweise überraschende Ergebnisse wurden in der Gruppe von Dr. Rullière zusammen mit seinem Laserexperten Gediminas Jonusauskas erzielt, denen ich nicht nur für die wissenschaftliche Zusammenarbeit danken möchte, sondern insbesondere für die äußerst herzliche Betreuung. Die Wochenendausflüge mit Claude und seinen wissenschaftlichen Gästen werde ich immer in lebhafter Erinnerung behalten. Viel Spaß hatte ich auch mit allen Mitarbeitern von Claude, insbesondere mit Emmanuelle dem Weinexperten, der auch im Squash gar nicht so schlecht war.

Bei Prof. F.C. DeSchryver möchte ich mich dafür bedanken, daß ich an „seinen“ Phenanthren Derivaten mitarbeiten durfte, wodurch ich viele interessante Erkenntnisse gewinnen konnte.

Bei Knut Rurack bedanke ich mich für wertvolle Kommentare, insbesondere zu seinem Spezialgebiet der Fluoreszenzsonden, nachdem er sich durch einige Seiten meiner Dissertation und „Monstersätze“ durchgeschlagen hatte.

Herrn Dr. Moritz danke ich für die Hilfsbereitschaft, mir eine funktionstüchtige pH Glaselektrode zur Verfügung zu stellen.

Thanks to Dr. Murthy S. Gudipati who always had time to discuss and to give valuable and sometimes philosophic advices.

Der Werkstatt des Ivan-N. Stranski Instituts als auch des Walther Nernst Instituts danke ich für die unkomplizierte Umsetzung meiner Anfragen.

Mein besonderer Dank gilt Anja, die mich in der entscheidenden Phase von allen täglichen Pflichten befreit hat und mich auch ansonsten voll unterstützt hat. Obwohl sie es noch nicht wahrnehmen können, danke ich auch Sara und Janina, die mich immer bei guter

Laune gehalten haben und im übrigen nie einen Zweifel daran gelassen haben, wer die neuen „Herrscher“ im Haus sind.

Wir können einem Menschen verzeihen, daß er etwas Nützliches schafft, solange er es nicht bewundert. Die einzige Entschuldigung dafür, etwas Nutzloses zu schaffen, besteht darin, daß man es über jedes Maß bewundert.

*Oscar Wilde*

Wenn man dir liniertes Papier gibt, schreibe quer über die Zeilen.

*Juan Ramón Jiminéz*

## Zusammenfassung

### Photoinduzierter intramolekularer Ladungstransfer in Donor-Akzeptor Biarylen und daraus resultierende Anwendungsaspekte in Hinsicht auf Fluoreszenzsonden und Solarenergieumwandlung

Im Mittelpunkt der vorliegenden Arbeit stehen die Untersuchungen des photoinduzierten intramolekularen Ladungstransfer in drei unterschiedlich verdrillten Donor-Akzeptor (D-A) Biphenylen. Unter Zuhilfenahme eines weiteren Paares unterschiedlich verdrillter D-A Biaryle werden dabei zum einen allgemeine Erkenntnisse zum photoinduzierten Verhalten von D-A Biarylen gewonnen und zum anderen mögliche Anwendungen in Bereichen der Solarenergienutzung und der Sondierung von Mikroumgebungen mittels Fluoreszenz diskutiert.

Neben experimentellen Methoden der stationären und zeitaufgelösten (ps bis s) Lumineszenz, transienten Absorption (sub-ps), Polarisationspektroskopie, Hochdruck- und Tieftemperaturtechnik kommen quantenchemische Rechnungen zum Einsatz.

Die elektronischen Zustände der D-A Biaryle können durch die Wechselwirkungen der Elektronenzustände der jeweiligen Arylhälften beschrieben und den beobachteten Absorptionsbanden zugeordnet werden. Elektronentransferwechselwirkungen (D→A) führen zu einer tief liegenden, intramolekularen Charge Transfer (CT) Bande, die aufgrund der starken Kopplung des reinen Elektronentransferzustandes mit dem Grund- ( $S_0$ ) und  $^1L_a$ -Zustand sehr intensiv ist. Der photoinduzierte intramolekulare Ladungstransfer weist sich durch stark solvatochrome Fluoreszenz aus, wobei das daraus abgeleitete Dipolmoment mit dem Verdrillungswinkel zunimmt. Überraschenderweise wird nach optischer CT Anregung der D-A Biphenyle zunächst ein unpolarer  $\pi\pi^*$  Zustand (mit  $^1FC$  bezeichnet) besetzt, bevor der Elektronentransfer in wenigen Pikosekunden von der Dimethylanilin- zur Benzonitrileinheit stattfindet. Die im Verhältnis zur Solvensrelaxation langsame und durch die im Mutter-Tochter Verhältnis stehende duale Fluoreszenzverstärkung eindeutig verfolgbare Elektronentransferreaktion wird auf eine interne conversion zwischen zwei schwach miteinander wechselwirkenden Zuständen zurückgeführt, die in erster Näherung unterschiedliche Symmetrien besitzen.

Wie schon für das unsubstituierte Biphenyl bekannt, deuten die transienten Absorptionsspektren und quantenchemischen Rechnungen eine photoinduzierte initiale Relaxation zu einer stärker planaren Konformation als im  $S_0$  an. Die Analyse der elektronischen Übergangsdipolmomente aus Absorption, Fluoreszenz und semiempirischen Berechnungen zeigen, daß das flexible D-A Biphenyl (**II**) im  $^1CT$  Zustand seine planare Konformation unabhängig von der Lösungsmittelpolarität beibehält. Das durch zwei Methylgruppen in ortho Position substituierte stark verdrillte D-A Biphenyl (**III**) bleibt im  $^1CT$  nur in unpolaren Lösungsmitteln planarer als in  $S_0$ , während es in stark polaren Lösungsmitteln stärker verdrillt in  $^1CT$  als im  $S_0$  vorliegt. Dafür gibt es weitere Anzeichen, wie z.B. die Tatsache, daß das ausrelaxierte transiente Absorptionsspektrum dem der Summe aus Dimethylanilin Kation und Benzonitril Anion entspricht als auch die Beobachtung, daß nur



die  $^1\text{CT}$  Fluoreszenz von **III** durch Wasserstoffbrückenbindungen gelöscht wird; beides ist mit einer biradikaloiden stark ladungstrennten Elektronenstruktur, induziert durch eine stark verdrillte Konformation, erklärbar. In mittelpolaren Lösungsmitteln liegt für **III** ein Gleichgewicht zwischen dem planarerem (**CT**) und verdrillteren Konformer (**CTR**) vor, welches für das Lösungsmittel Diethylether mittels temperaturabhängiger Globalanalyse von Fluoreszenzabklingkurven thermodynamisch und kinetisch quantitativ charakterisiert wird. Eine hohe Aktivierungsenergie ( $E_a=14$  kJ/mol) ist verantwortlich für eine im Verhältnis zum Dimethylaminobenzonitril (DMABN) relativ langsame adiabatische Photoreaktion von der planarerem Spezies **CT** hin zu der verdrillteren, weiter relaxierten Spezies **CTR** mit größerem Elektronentransfer Charakter. Durch den Vergleich von druck- mit temperaturabhängigen Fluoreszenzmessungen kann geschlossen werden, daß tatsächlich eine thermische, d.h. intrinsische Barriere vorliegt und die Photoreaktion zusätzlich viskositätskontrolliert ist.

Die Eignung der D-A Biphenyle als Fluoreszenzsonden für Mikropolarität, sich stark ändernde Mikroviskosität oder Matrixordnung, für protische Lösungsmittel und pH wird untersucht. Die komplementären Sondereigenschaften von **II** und **III** werden herausgestellt und die mit dem Sondenprozeß verbundenen Mechanismen diskutiert. Insbesondere die Fluoreszenzsondierung des pH erscheint als ein vielversprechendes Anwendungsfeld.

Die ungewöhnliche Eigenschaft von planaren oder mäßig verdrillten D-A Biarylen, hohe Fluoreszenzquantenausbeuten mit großen Dipolmomenten und daraus resultierenden großen Stokes-shifts zu kombinieren wird demonstriert und zur Nutzung in Fluoreszenzsolar-konzentratoren vorgeschlagen. Andererseits bieten stark verdrillte D-A Biaryle durch ihre nahezu ladungstrennte Elektronenstruktur im angeregten Zustand die Möglichkeit, über intermolekularen Elektronentransfer photokatalytisch zu wirken. Entsprechende Perspektiven für die photochemische Nutzung der Solarenergie werden kurz diskutiert und aufgezeigt.

## Abstract

### Photoinduced Intramolecular Charge Transfer in Donor-Acceptor Biaryls and Resulting Applicational Aspects Regarding Fluorescent Probes and Solar Energy Conversion

This study is focused on the effects of photoinduced intramolecular charge transfer (CT) in three differently twisted donor-acceptor (D-A) biphenyls. Taking into account another pair of differently twisted D-A biaryls new universal insights into the photoinduced electronic and conformation dynamics of D-A biaryls are obtained. Furthermore, possible applications in fields of solar energy conversion and fluorescence sensing of microenvironments are demonstrated.

Experimental means of stationary and time-resolved (ps to s) luminescence, transient absorption (sub-ps), polarization spectroscopy, high pressure and low temperature techniques are employed in conjunction with quantum chemical calculations.

Twist angle and solvent dependent electron transfer (ET) interactions between the D and A aryl moieties are responsible for the low lying and solvatochromic intramolecular CT electron band which gains unusually high intensity through strong electronic coupling of the pure  $^1\text{ET}$  with the ground ( $S_0$ ) and  $^1L_a$  state. As regards the class of biaryl compounds, for the first time, an excited state electron transfer from the D to the A could be monitored by dual spectrally separated stimulated fluorescence bands with precursor-successor relationship on a sub-ps timescale for the D-A biphenyls. It is concluded that, in addition to the electronic interaction of  $^1\text{ET}$  with  $S_0$  and  $^1L_a$ , the electronic interaction with a close lying  $^1L_b$  state plays a fundamental role in the ET dynamics and the  $^1\text{CT-S}_0$  transition probability in D-A biaryls.

The initial photoinduced conformational relaxation occurs towards planarity in all biaryls investigated. However, various results evidence that the highly twisted D-A biphenyl additionally performs a slow "excited state intramolecular back twist rotation" leading to a solvent polarity dependent conformational equilibrium between a more planar (**CT**) and a more twisted (**CTR**) conformer in  $S_1(^1\text{CT})$ . Using global analysis of the biexponential fluorescence decays as a function of temperature and pressure in medium polar solvents, the kinetics, thermodynamics, viscosity control and decomposed emission spectra associated with this adiabatic photoreaction are determined.

The twist angle dependent ability of the D-A biphenyls to serve as fluorescent probes of micropolarity, changes of microviscosity or matrix order, protic solvents and pH is investigated. In particular, fluorescence sensing of pH seems to be promising.

The advantageous property of planar or moderately twisted D-A biaryls to combine high fluorescence quantum yields with large Stokes-shifts is proposed for the use in fluorescent solar concentrators. Alternatively, almost full charge separation in  $S_1$  of strongly twisted D-A biaryls provides the possibility of electron transfer initiated photocatalysis.

# Contents

Danksagungen

Zusammenfassung

Abstract

<b>Chapter 1</b>	<b>Introduction</b>	<b>1</b>
	Goals, text guide and nomenclature	1
<b>Chapter 2</b>	<b>Absorption Spectra and Electronic Structure of D-A Biphenyls</b>	<b>4</b>
	2.1 Introduction	4
	2.2 Experimental	5
	2.3 Results and Discussion	6
	2.3.1 Composite molecule approach for donor-acceptor biphenyls I-III	6
	2.3.2 UV/VIS absorption spectra and their derivatives	10
	2.3.3 Linear dichroic absorption spectra	13
	2.3.4 Comparison of spectral data with calculated results	14
	2.4 Conclusions	16
	2.5 References	16
<b>Chapter 3</b>	<b>Fluorescence and Photophysics of D-A Biphenyls at 298 K</b>	<b>18</b>
	3.1 Introduction	18
	3.2 Experimental Section	21
	3.2.1 Synthesis of the compounds	21
	3.2.2 Solvents	21
	3.2.3 Steady state absorption	21
	3.2.4 Steady state fluorescence	22
	3.2.5 Fluorescence quantum yields	22
	3.2.6 Fluorescence lifetimes	22
	3.2.7 Quantum chemical calculations	23
	3.3 Results and Discussion	24
	3.3.1 Steady state spectra	24
	3.3.2 Excited state dipole moments from solvatochromic plots	29
	3.3.3 Photophysics	32
	3.3.3.1 Photophysical evidence for $^1L_a$ -type fluorescence	32
	3.3.3.2 Structural and solvent dependence of nonradiative rates	33
	3.3.3.3 Ratios of radiative rate constants as indicators for angular relaxations	36
	3.3.3.4 Excited state conformational equilibrium for III	38
	3.3.4 Theoretical calculations	40
	3.3.4.1 Twist potentials in $S_0$	40
	3.3.4.2 Electronic nature of $S_1$	42
	3.3.4.3 Molecular structure in $S_1$	43
	3.4 Conclusions	47
	3.5 References and Notes	49
<b>Chapter 4</b>	<b>Sub-picosecond Transient Absorption of D-A Biphenyls. Intramolecular Control of the Excited State Charge Transfer Processes.</b>	<b>52</b>
	4.1 Introduction	52
	4.2 Experimental	55
	4.2.1 Materials	55
	4.2.2 Picosecond pump-probe experiments	55
	4.2.3 Correction and fitting of the results	55
	4.2.4 Quantum chemical calculation of the transient spectra	56
	4.3 Results	57

4.3.1	Steady-state spectra and expectations	57
4.3.2	Transient absorption measurements	58
4.3.2.1	n-Hexane solutions	59
4.3.2.2	Acetonitrile solutions	60
4.3.2.3	Diethylether solutions	62
4.3.2.4	Triacetone solutions	64
4.4	Discussion	67
4.4.1	Excited state absorption and gain bands	67
4.4.1.1	Assignments of the absorbing and emitting species to two states	67
4.4.1.2	Effects of solvent polarity and twist angle	68
4.4.2	Structural relaxation	71
4.4.3	Kinetics of state interconversion $^1FC \rightarrow ^1CT$	74
4.5	Conclusions	77
4.6	References	79
<b>Chapter 5</b>	<b>Fluorescence Polarization Spectroscopy of D-A Biphenyls at 77K. The Electronic Relaxations.</b>	<b>81</b>
5.1	Introduction	81
5.2	Experimental	82
5.2.1	Polarization and millisecond luminescence spectroscopy	82
5.3	Results and Discussion	82
5.4	References	88
<b>Chapter 6</b>	<b>Temperature Dependent Study of Excited State Conformational Relaxations in D-A Biphenyls Using Steady-State and Time-Resolved Fluorescence</b>	<b>89</b>
6.1	Introduction	89
6.2	Experimental	91
6.2.1	Low temperature measurements	92
6.2.2	Band shape analysis	92
6.2.3	Global analysis of emission decays	92
6.3	Results and Discussion	93
6.3.1	Temperature dependence of radiative back charge transfer and excited state relaxations for the D-A biphenyls I-III.	93
6.3.1.1	Energetics from fluorescence band shape analysis	93
6.3.1.2	Analysis of the fluorescence lifetimes and quantum yields.	97
6.3.2	Temperature dependence of the conformational equilibrium in the excited state $^1CT$ of the strongly pretwisted D-A biphenyl III in diethylether	101
6.3.2.1	The method to recover dual fluorescence bands and to derive the reaction rate constants by global analysis of emission decays	101
6.3.2.2	Quantitative characterization of the excited state conformational equilibrium between two charge transfer species CT and CTR	106
6.4	Conclusion	111
6.5	References and Notes	112
<b>Chapter 7</b>	<b>Pressure and Temperature Dependent Fluorescence of D-A Biphenyls. The Separation of Viscosity and Thermal Control of the Conformational Photoreaction in the Highly Twisted Compound</b>	<b>114</b>
7.1	Introduction	114
7.2	Experimental	116
7.2.1	High pressure equipment	116
7.2.2	Ti:Sapphire Laser	116
7.3	Results and Discussion	116
7.3.1	Viscosity and temperature influence on the fluorescence and excited state relaxations of I-III in triacetone (TAC).	116
7.3.2	Analysis of reaction rate constants and its boundary conditions	119
7.3.3	The method to distinguish between viscosity and thermal control of a photoreaction	123
7.3.4	Separated thermal activation energy and viscosity dependence of the conformational photoreaction in III.	125

7.4 Concluding Remarks	128
7.5 References	129
<b>Chapter 8 The Influence of Conformation and Energy Gaps on Optical Transition Moments in D-A Biphenyls..</b>	<b>130</b>
8.1 Introduction	131
8.2 Experimental and Semiempirical Calculations	132
8.3 Results and Discussion	132
8.3.1 Experimental transition dipole moments	132
8.3.2 Electronic coupling between $^1\text{ET}$ and $^1\text{L}_a$ in dependence of the twist-angle	133
8.3.3 Description of transition moments with reference states	135
8.3.4 Influence of structural relaxations other than $\varphi_{\text{D-A}}$ twisting on $M_{\text{CT}}$	138
8.3.5 Influence of the $^1\text{ET}$ - $^1\text{L}_a$ energy gap on $M_{\text{CT}}$	139
8.3.6 Evaluation of $S_0$ and $S_1$ twist angles in solvents	143
8.4 Concluding Remarks	143
8.5 References and Notes	144
<b>Chapter 9 Conformation and Energy Gap Dependent Electron Transfer Interactions in Flexible D-A Biaryls: The Case of Two Twisted 9-(dimethylanilino) phenanthrenes</b>	<b>146</b>
9.1 Introduction	146
9.2 Experimental and Calculations	147
9.3 Results	148
9.3.1 Spectroscopic transition moments and energies	148
9.3.2 Quantum chemical calculations	151
9.4 Discussion	154
9.4.1 Influence of electron transfer interactions on absorption and emission bands.	154
9.4.2 Squared transition moments as indicators for molecular and electronic structure	154
9.5 Conclusions	158
9.6 References and Notes	159
<b>Chapter 10 Possible Applications of D-A Biphenyls as Fluorescent Probes</b>	<b>160</b>
10.1 Introduction	160
10.2 Experimental	163
10.2.1 Measurements of pH	163
10.3 Results and Discussion	163
10.3.1 Micropolarity	163
10.3.2 Transition temperature from liquid to solid ( $T_g$ )	165
10.3.3 Protic solvents	170
10.3.4 Sensitive and self-calibrating sensing of pH in aqueous solution	174
10.4 Conclusion	182
10.5 References and Notes	182
<b>Chapter 11 Implications to Solar Energy Conversion</b>	<b>186</b>
11.1 Introduction	186
11.2 Experimental	188
11.2.1 Preparation of polymer films	188
11.3 Results and Discussion	189
11.3.1 Requirements for low lying and highly fluorescent $^1\text{CT}$ states in D-A biaryls	189
11.3.2 Which host environment is favourable for Fluorescent Solar Concentrators (FSC)	191
11.4 Solar Perspectives	196
11.4.1 Fluorescent Solar Concentrators using planar or moderately twisted D-A biaryls	196
11.4.2 Towards Electron Transfer Initiated Photocatalysis (ETIP) using twisted D-A biaryls	197
11.5 References	
<b>Chapter 12 Final Conclusions</b>	<b>200</b>

**Appendix A**  
**Glossary of Abbreviations**  
**List of Publications**  
**Lebenslauf**

# Chapter 1

## Introduction

This introductory chapter aims to point out the general goal of the whole work and to serve as a guide through all chapters. It is NOT an introduction to the specific field investigated. Each chapter consists of its own introduction giving the important information of the method employed (usually in the results and discussion section) and a report of the state of the art. An overview regarding the class of donor-acceptor biphenyls is given in Ch. 3.1 with more photophysical details in 3.3.

### Goals

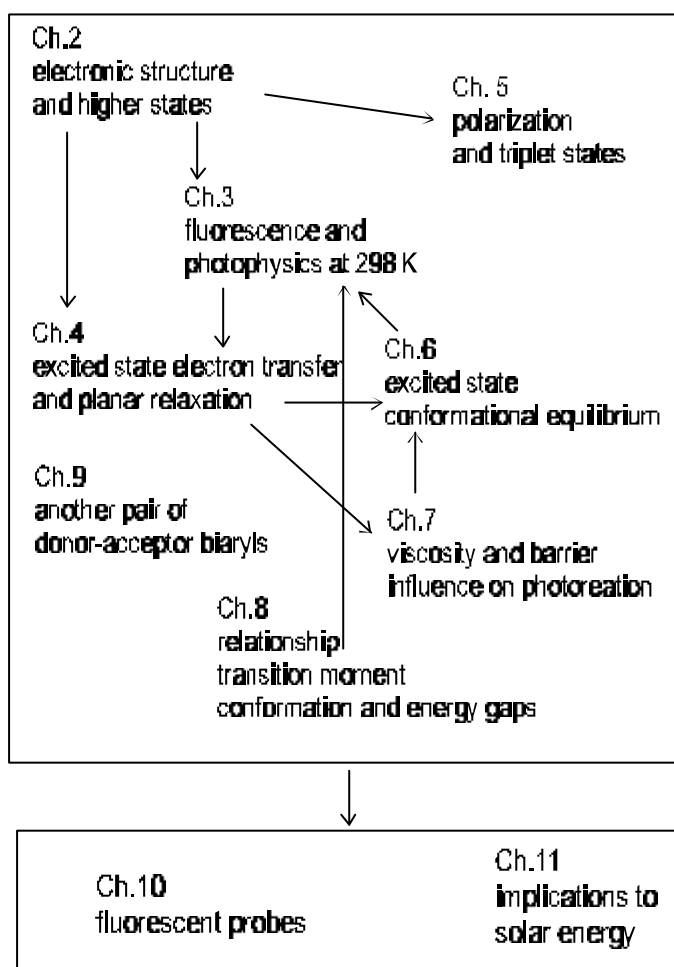
In view of a common goal to exploit light using *photon-driven molecular devices* (PMD), e.g. solar energy converters or microsensors, science fulfills the task on the one hand, *to investigate and characterize possible candidates* of PMD's and, on the other hand, to analyze the applied basic principles and mechanisms utilizing model compounds in order *to provide a theoretical platform* necessary to improve existing and complex PMD's.

The current study intends to give a contribution to both but with a main stress on the second item, i.e. the investigation of a promising photoinduced mechanism with model compounds. The photon-induced process studied is *intramolecular charge transfer* between two well-defined molecular fragments of controllable electronic interaction. The model compounds are three donor-acceptor biphenyls where the electron pushing dimethylanilino groups (D) are attached by a single chemical bond to the electron pulling benzonitrile groups (A) in a different spatial arrangement modified by the twist angle ( $\varphi_{D-A}$ ) between the planes of both moieties.

Since the model compounds were synthesized and investigated for the first time (except compound **II** which was simultaneously investigated by F.Lahmani/Orsay Cedex in a different way) a large part of this Ph.D. thesis deals with the electronic and photophysical characterization of the compounds in order to derive the photon-induced intramolecular electronic and conformational relaxations. Furthermore, using this knowledge advanced contemporary methods to analyze charge transfer processes are applied and evaluated. Finally, possible applications of photoinduced *intramolecular charge transfer* in donor-acceptor biphenyls, or more commonly in biaryls, as PMD's in the field of solar energy conversion and microenvironmental sensing are principally discussed and partially demonstrated.

## Text Structure and Guide

Scheme 1.1 illustrates the structure of the text and the arrows denote the flow of information needed to reach the conclusions in the relevant chapter. In ch. 2, the absorption spectra are



**Scheme 1.1** Flow diagram of text organization

analyzed and the electronic structure is interpreted in terms of a composite-molecule model. In ch. 3, the fluorescence is investigated and the electronic nature of the emitting state is analyzed. It gives a survey about the photophysics at room temperature. The conclusions in ch. 3 are substantiated by more detailed results given in the following chapters. Ch 3 may be regarded as the heart of the text structure giving the references to the parts where more details can be found. For example, the transient absorption experiments in ch. 4 indicate an initial relaxation towards planarity, ch. 5 is focused on the triplet behaviour, ch. 6 and 7 provide a detailed description of the excited state equilibrium and ch. 8 analyzes the solvent and conformation dependent transition moments. To address the question whether the derived photoinduced properties can be transferred to larger biaryl systems, two differently twisted phenanthryl derivatives are examined in ch. 9 analogously to **I-III**. All these informations are finally used to discuss and demonstrate aspects of possible applications regarding fluorescence sensing (ch.10) and solar energy conversion (ch. 11).



### Comments to Nomenclature

The recommendations of the GLOSSARY OF TERMS IN PHOTOCHEMISTRY (GOTIP) [Pure & Appl. Chem. 1988, 60, 1055-1106.] are followed. The most important differentiation to be noted is the distinguished use of intramolecular charge transfer (CT) and intramolecular electron transfer (ET). Here and in the GOTIP, CT denotes the transfer of a FRACTION of electronic charge between localized sites in a molecule, while ET stands for the FULL transfer of one electron ( $=1.602 \times 10^{-19} \text{C}$ ) between the relevant sites or units.

Note one exception of GOTIP notation: The preferred energy unit here is the wavenumber in  $\text{cm}^{-1}$  which is abbreviated here by  $\nu$  without the usual queue.

## Chapter 2

# Absorption Spectra and Electronic Structure of D-A Biphenyls

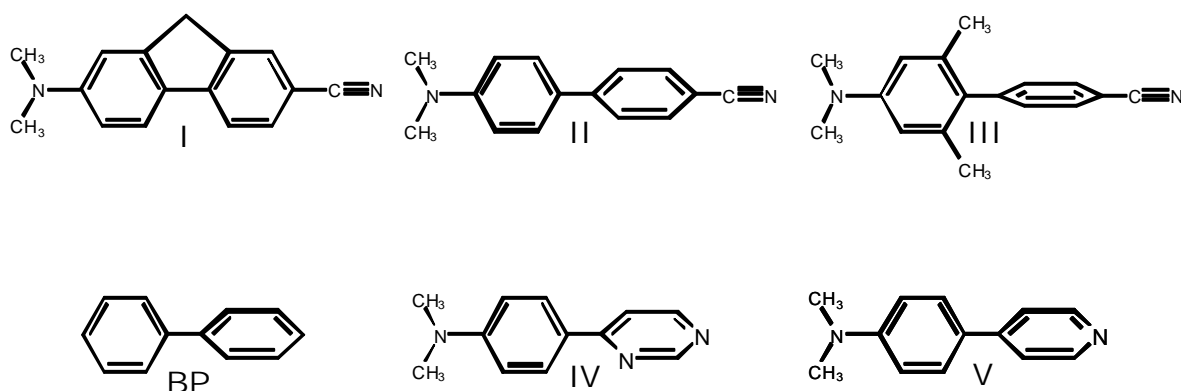
### Abstract

The electronic structure of 4-(*N,N*-Dimethylamino)-4'-cyano-biphenyl and its planar fluorene and twisted 2,6-dimethyl-substituted model compounds (**I-III**) is analyzed by experimental means of UV/VIS absorption spectroscopy including linear dichroic and derivative spectra. CNDO/S-CI calculations show that the electronic structure of the biphenyls investigated can be approximately described within a composite-molecule model based on the  ${}^1L_b$ ,  ${}^1L_a$  states of the dimethylaniline and benzonitrile subunits. But in addition to unsubstituted biphenyl (BP), an intramolecular charge transfer ( ${}^1CT$ ) state is active as the first excited singlet state and the twist angle dependent interaction with the higher lying, locally excited singlet states modifies the absorption spectra. The A, B, C and H absorption bands of unsubstituted biphenyl can be correlated with the absorption spectra of the donor-acceptor biphenyls **I-III** and the additional absorption band at fairly lower energy than the A band in biphenyl is assigned to a strong intramolecular CT band. This leads to a consistent and helpful interpretation of the electronic structure of donor-acceptor biphenyls including those (**IV-V**) investigated already in literature.

**Keywords:** biphenyl, UV/VIS absorption, linear dichroism, CNDO/S, electronic structure

## 2.1 Introduction

For the unsubstituted biphenyl (**BP**), several theoretical publications confirmed the correlation of the electronic states with states derived from the composite molecule model.<sup>1-4</sup> But in contrast to **BP**, in series of 4,4'-donor-acceptor substituted biphenyls charge transfer excitations cannot be neglected.



Until recently, a number of publications dealt with charge transfer properties of donor-acceptor (D-A) biphenyls<sup>5-11</sup> but none of them gave an in-depth and uniform interpretation of the electronic structure. Particularly the biphenyl compounds **II**, **IV** and **V** have already been investigated.<sup>9-11</sup> It has been reported for these compounds that the first strong absorption band is due to a  ${}^1L_a$ -type state. HERBICH and WALUK<sup>10</sup> concluded that absorption and fluorescence of

**IV** originate from the same state containing partial charge transfer character of similar magnitude. On the other hand, LAHMANI ET AL.<sup>11</sup> proposed for compound **II** primary excitation to a locally excited state of the  $^1L_a$  type but radiative deactivation from a charge transfer state gaining intensity by mixing with locally excited states. Moreover, the involvement and assignments of the higher lying states was not investigated. BULGAREVICH ET AL.<sup>9</sup> gave assignments for the  $^1L_b$  and  $^1B_b$  states in the absorption spectrum of **V** but from the present investigation it follows that the  $^1L_b$  assignment was not correct.

In order to improve and complete the interpretation often given for absorption spectra of D-A biphenyls and because we need a good knowledge of the electronic properties of **I-III** for the following studies including time-resolved transient absorption<sup>12</sup> in ch. 4 and fluorescence<sup>13</sup> in ch. 3, it is necessary to have a closer look on the electronic structure of the D-A biphenyl **II**. The biphenyl series is supplemented with the planar and more twisted biphenyl compounds **I** and **III** and especially the comparison of **II** with these sterically restricted biphenyls **I** and **III** should enable us to unambiguously assign the observed electronic transitions in D-A biphenyls. This study sets the basis for the following experimental studies on the D-A biphenyl series **I-III**. Therefore, in this chapter the assignments of the relevant electronic states are given and it is shown that the electronic structure is nearly independent of the methyl substitution pattern in **I** and **III** and that the observed changes can be satisfactorily described by the influence of the twist angle in the biphenyl **II**.

## 2.2 Experimental

CNDO/S-SCI calculations including 49 singly excited configurations have been performed with the QCPE program #333 modified to use the original CNDO/S parametrization<sup>14</sup> and to calculate the excited state dipole moments. All input geometries were fully optimized in the ground state by the Newton algorithm with the AM1 Hamiltonian within the AMPAC program.<sup>15</sup> All quantum chemical calculations were executed on a HP 735 workstation.

The synthesis of the compounds **I-III** is described in ch. 3.<sup>13</sup>

All solvents used were of spectroscopic grade (Merck UVASOL) and the commercial polyethylene sheets have been checked for impurities by absorption and fluorescence. The absorption spectra presented were recorded on a ATI UNICAM UV4 UV/VIS spectrophotometer and the decadic molar extinction coefficients  $\epsilon$  were repeatedly determined. The linear dichroic spectra have been obtained using a conventional arrangement<sup>16,17</sup> with a rotatable UV-Glan-Thomson polarizer and fixed stretched polyethylene sheets inside the ATI spectrophotometer.

## 2.3 Results and Discussion

### 2.3.1 Composite Molecule Approach for Donor-Acceptor Biphenyls I-III

In order to confidently treat the electronic structure of a super-molecule consisting of two different chromophoric parts in terms of a composite-molecule model<sup>18</sup> it is necessary to have a substantial localization of the molecular orbitals (MOs) on each subunit. Within the LHM method developed by LONGUET-HIGGINS and MURRELL,<sup>19,20</sup> this precondition is assumed per sé since it uses only localized MOs. The configuration interaction (CI) calculation then yields final wavefunctions for the electronic states which can readily be interpreted in terms of the composite fragments. An alternative procedure using delocalized MOs has been proposed by BABA, SUZUKI and TAKEMURA.<sup>21</sup> In their original work, they applied the Pariser-Parr-Pople (PPP) method<sup>22</sup> including a CI calculation. A configuration analysis was then performed to interpret the results in the language of the more comprehensible composite-molecule model.

In this work, the method of BABA, SUZUKI and TAKEMURA is principally followed but instead of the PPP method the more sophisticated CNDO/S<sup>14</sup> method is employed. A brief outline of our configuration analysis method is given in the Appendix A. In Fig. 2.1a, the most important MOs obtained for the separated phenyl-subunits dimethylaniline (donor part D) and benzonitrile (acceptor part A) as well as for the composite biphenyl molecule **II** (D-A) at three different twist angles are depicted. Using Platt's notation,<sup>23</sup> the one-electron configurations responsible for the  $^1L_b$  and  $^1L_a$  states of the free donor and acceptor molecules are indicated. As one can see, at 90° twist of the donor and acceptor phenyl part in the composite molecule, the MOs are effectively localized on the subchromophors and correspond to the MOs of the free donor and acceptor part. This is also substantiated by the retained MO energies and symmetries. As a consequence, in the composite molecule at 90°, the same local  $^1L_b$  and  $^1L_a$  transitions are active as in the separated D and A parts. Transitions between the subunits (electron transfer) are forbidden at 90° due to vanishing overlap of the donor and acceptor MOs. Deviations from perpendicularity reduce the symmetry of the molecule from  $C_{2v}$  to  $C_2$  and thus lead to interactions between MOs of equal symmetry (Fig. 2.1a). Nevertheless, even at full planarity the MOs keep substantial localized character which gives the justification to continue the classification of localized  $^1L_b$  and  $^1L_a$  transitions. The strongest interactions occur between the occupied MOs 1 and 2 and the unoccupied MOs -1 and -4 (all of equal MO symmetry B) resulting in two important consequences for the HOMO-LUMO configuration:

- 1) The HOMO-LUMO transition is of pure electron transfer character at 90°, but at non-perpendicular twist angles the MO mixing dilutes the electron transfer character and introduces partial  $L_a(D)$  and  $L_a(A)$  character. Tab. 2.1 shows that the electron transfer (ET) character of the

HOMO-LUMO transition decreases from 96% at 90° to 42% at 0° accompanied by an increase of 4%  $^1L_a$ -type contributions at 90° up to 46% at 0°. Nevertheless, even at 0°, the ET contribution (HOMO(D)→LUMO(A) of the localized units) is by far largest for the state ( $2^1A$ ) connected with around 90% (see below Tab. 2.2) of the HOMO-LUMO transition. Due to the strong ET character of  $2^1A$  this state is called the intramolecular charge transfer state  $^1CT$  to account for its sizeable charge separation between the phenyl units. This is also verified by the large dipole moments of the  $^1CT$  state as compared to the other states calculated (see below Tab. 2.4).

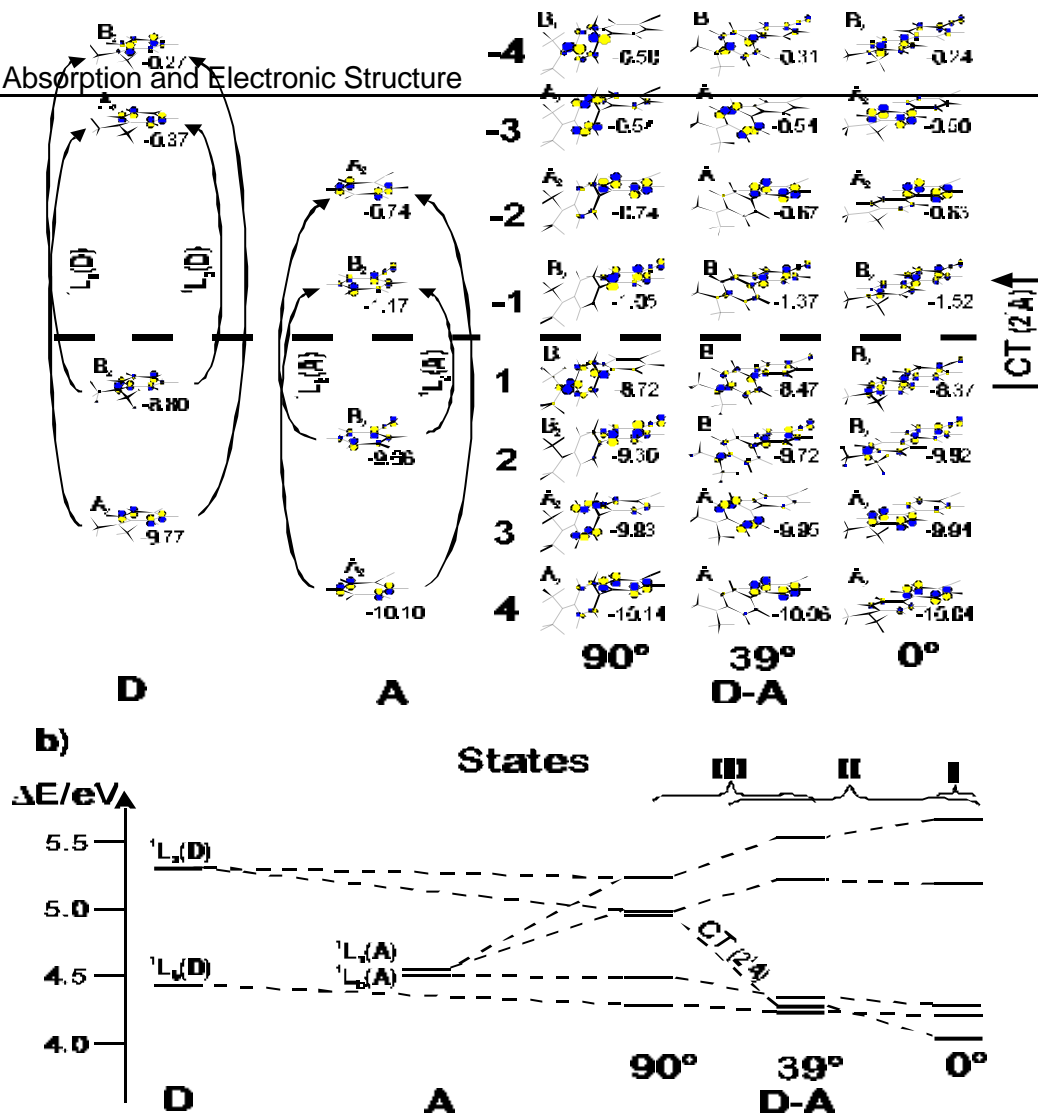


**Fig. 2.1** a) Calculated molecular orbitals of dimethylaniline (D), benzonitrile (A) and **II** (D-A) at 0°, 39° and 90°. MO energies (in eV) and MO symmetries (within molecular symmetry  $C_{2v}$  for 0° and 90° and  $C_2$  for intermediate angle 39°) are also given.

b) Correlation diagram for the singlet state transitions of dimethylaniline (D) and benzonitrile (A) in regard to the composite molecule **II**. The braces indicate the available twist angle regions for each of the D-A biphenyls

2) The increased MO interaction with increasing planarity also leads to a reduced HOMO-LUMO gap and therefore to a stabilization of the  $^1CT$  state. The ensuing twist angle dependent transition energy is well reflected by the correlation diagram shown in Fig. 2.1b. By changing the spatial arrangement of the donor and acceptor phenyl units from perpendicularity to planarity, the charge transfer state gets stabilized by 0.9 eV ( $7300 \text{ cm}^{-1}$ ). This means that in contrast to the high lying  $^1CT$  state in unsubstituted biphenyl **BP**, the  $^1CT$  state of the D-A biphenyl **II** can become the lowest excited singlet state even in the gas phase for twist angles less than 39°.

Moreover, Fig. 2.1b shows that, similar to **BP**,<sup>2</sup> the interaction between the  $^1L_b$  states is weak due to their small transition moments, so that they nearly retain their transition energies with respect to the free subunits and exhibit only a slight stabilization with increasing planarity. The fact that the stabilization of the  $^1CT$  state is much stronger than that of the  $^1L_b$  state suggests a quite stronger tendency of the D-A biphenyl **II** for a structural relaxation to planarity in the excited state than it was observed for **BP** itself.<sup>24-27</sup> In fact, an excited state relaxation towards planarity for **II** (and **III** only in non-polar solvents) in the excited state is concluded from time-resolved fluorescence measurements (ch. 3)<sup>13,28,29</sup> Similar as for **BP**,<sup>2,4</sup> the interaction between the more allowed local  $^1L_a$ -states is much stronger. In **BP**, the enhanced interaction is reflected by a larger energy splitting between the out-of-phase and in-phase linear combination of the local  $^1L_a$  excitations of equal energy. The strong interaction between the non-degenerate  $^1L_a$  states in the D-A biphenyls is testified by a nearly 50:50 mixing of the donor and acceptor  $^1L_a$  configurations in the present calculation. A comparable enhancement of the energy splitting between the  $^1L_a$  states as in **BP**<sup>2</sup> is observed with decreasing twist angle (Fig. 2.1b). The most important differences to **BP** result from the additional interaction of the  $^1L_a$  states with the low lying charge transfer state. All three states possess the same symmetry ( $^1A$  within  $C_2$ ) with polarization in the long molecular axis. The interaction between these states increases with decreasing twist angle and partly accounts for the stabilization of the  $^1CT$  state at the cost of destabilization of the  $^1L_a$  states, as well as for the decreasing oscillator strengths of  $^1L_a$  with decreasing twist angle. Thus, for the absorption spectra of **I-III** we have to expect an inverse behaviour of the  $^1L_a$  band as it is observed for **BP**. For **BP**, it is well-known that with increasing twist angle the energy of the  $^1L_a$  band shifts hypsochromically accompanied with a loss of intensity.<sup>18,30-34</sup> For the D-A biphenyls studied here, the behaviour of the  $^1L_a$  band in **BP** is

**Tab. 2.1** Local ( $L_a$  or  $B_a$ ) and Electron Transfer (ET and Reverse ET) Character of the Delocalized HOMO-LUMO ( $1 \rightarrow -1$ ) Configuration. The Values for the Model Compounds **I** at  $0^\circ$  and **III** at  $40^\circ$  and  $90^\circ$  are Given in Brackets.

angle	$L_a(D)$	$L_a(A)$	ET( $D^+A^-$ )	RET( $D^+A^+$ )
$90^\circ$	1.2% (1.2%)	3.2% (3.5%)	96% (95%)	0.04% (0.04%)
$39^\circ$	20% (16%)	22% (24%)	50% (53%)	9% (7%)
$0^\circ$	22% (21%)	24% (25%)	42% (41%)	13% (13%)

\* The data are derived from the coefficients of the  $2p\pi$  atomic orbitals (eq. A-2) in Appendix A) involved in the  $1 \rightarrow -1$  configuration. Because mixing between MOs of different symmetry is negligible, there is no  $L_b$  character in  $1 \rightarrow -1$ . predicted to be transferred to the CT absorption band.

Let us now discuss whether the electronic structure of the planar fluorene **I** and the more twisted biphenyl model compound **III** can approximately be described by that of **II**. The configuration analysis shows that the MOs are only very weakly affected by the methyl substitution pattern in **I** and **III** yielding the same configurations as for **II**. As an example, Tab. 2.1 shows that the character of the HOMO-LUMO ( $1 \rightarrow -1$ ) transition only depends on the twist

angle but not on the methyl substitution pattern. In detail, the percentages of the character for the HOMO-LUMO configuration are nearly identical for **II** and its model compounds **I** and **III** the values of which are given in brackets in Tab. 2.1. Further, in Tab. 2.2 the contributions of the characteristic configurations (see Fig. 2.1) to the charge transfer and the first four locally excited singlet states are compared for **II** with **I** and **III**. Independent of the compound and the twist angle, the  $^1\text{CT}$  state keeps the large  $1 \rightarrow -1$  contribution of about 90 % (with varying ET character, see Tab. 2.1). For **II** and **III**, the  $^1\text{L}_b$  and  $^1\text{L}_a$  assigned states are determined by similar weights of the contributions, too. Main differences are observed only between the contributions of **I** and **II**. The lower weights for **I** indicate more mixing between the states. This is not surprising since **I** is derived from unsubstituted fluorene which has  $C_{2v}$  symmetry with the twofold  $C_2$  symmetry axis perpendicular to that in **BP** which is of  $D_2$  symmetry with  $C_2$  along the long-molecular axis as in **II**. Therefore, in fluorene the benzene  $^1\text{L}_b$  (and  $^1\text{L}_a$ ) combinations split into a perpendicular and parallel polarized transition with respect to the long-molecular axis. The equal symmetry of the  $^1\text{L}_b(+)$  and  $^1\text{L}_a(-)$  states explains the enhanced mixing between these states in fluorene,<sup>2</sup> and can analogously explain the enhanced mixing behaviour of the D-A fluorene **I** (Tab. 2.2). This also leads to a relatively strong dependence of the calculated transition moment and its direction on the parametrization and geometry used for **I**.

**Tab. 2.2** Contributions (%) of the Characteristic Configurations to the  $^1\text{CT}$ ,  $^1\text{L}_b$ -type and  $^1\text{L}_a$ -type States. The Contribution to the  $^1\text{CT}$  State is Calculated by the Squared CI Coefficient of the  $1 \rightarrow -1$  Configuration and the Contributions to the  $^1\text{L}_b$  ( $^1\text{L}_a$ ) States are Calculated as the Sum of the Squared CI Coefficients of the Four  $^1\text{L}_b$  ( $^1\text{L}_a$ )-type Configurations Denoted in Fig. 2.1a (see eq. A-4 in Appendix A).

state	D	A	II / 90°	III / 90°	II / 39°	III / 40°	II / 0°	I / 0°
$^1\text{CT}(\text{D}^{\delta+}\text{A}^{\delta-})$	-	-	90%	89%	94%	92%	95%	83%
$^1\text{L}_b(\text{D})$ -type <sup>a</sup>	98%	-	90%	98%	74%	66%	61%	39%
$^1\text{L}_b(\text{A})$ -type <sup>a</sup>	-	98%	83%	98%	49%	59%	54%	50%
$^1\text{L}_a(\text{D})$ -type <sup>b</sup>	96%	-	96%	97%	91%	92%	88%	84%
$^1\text{L}_a(\text{A})$ -type <sup>b</sup>	-	34%	93%	94%	80%	45%	80%	27%

<sup>a</sup> The contributions to the two  $^1\text{L}_b$  states are mainly determined by the configurations of the respective subunit. Only for the  $^1\text{L}_b(\text{A})$  state at 0° for **I** and **II** the „wrong“  $^1\text{L}_b(\text{D})$  configuration contributions exceed 10%.

<sup>b</sup> Although the lower  $^1\text{L}_a$  state has more donor character, the donor and acceptor localized contributions are strongly mixed up to 50:50.

However, previous results show that the electronic structure of fluorene is better comparable with biphenyl than with molecules of equal  $C_{2v}$  symmetry like carbazole or phenanthrene<sup>35</sup> which have the short molecular axis as the symmetry axis  $C_2$ . The similarity of the relative CI contributions for **I** and **II**, and even better for **II** and **III** leads us to conclude that the electronic structure of **I** and **III** can approximately be described by that of **II** at the corresponding twist angles. In this case, the absorption spectra of **I-III** (and **IV-V**) should be interpretable with the calculation results obtained for **II**.

### 2.3.2 UV/VIS Absorption Spectra and Their Derivatives



In Fig. 2.2, the absorption spectra of **I-III** in the solvents n-hexane and acetonitrile are shown together with the calculated electronic transitions for **II** at 0°, 39° and 70° which are indicated by the column bars of length proportional to the respective oscillator strength (for more details see caption of Fig.2.2). It is common knowledge that without environment correction CNDO/S-CI calculations overestimate the transition energies even for non-polar aromatics in low-temperature matrices<sup>35,36</sup> by up to 5000 cm<sup>-1</sup>. Therefore, the positions of the column bars in Fig. 2.2 representing the calculated transitions are shifted 1700 cm<sup>-1</sup> to the red in order to give a better representation of the experimental spectra. For comparison, the INDO/S calculations previously published for compound **IV** also overestimated the transition energies of the

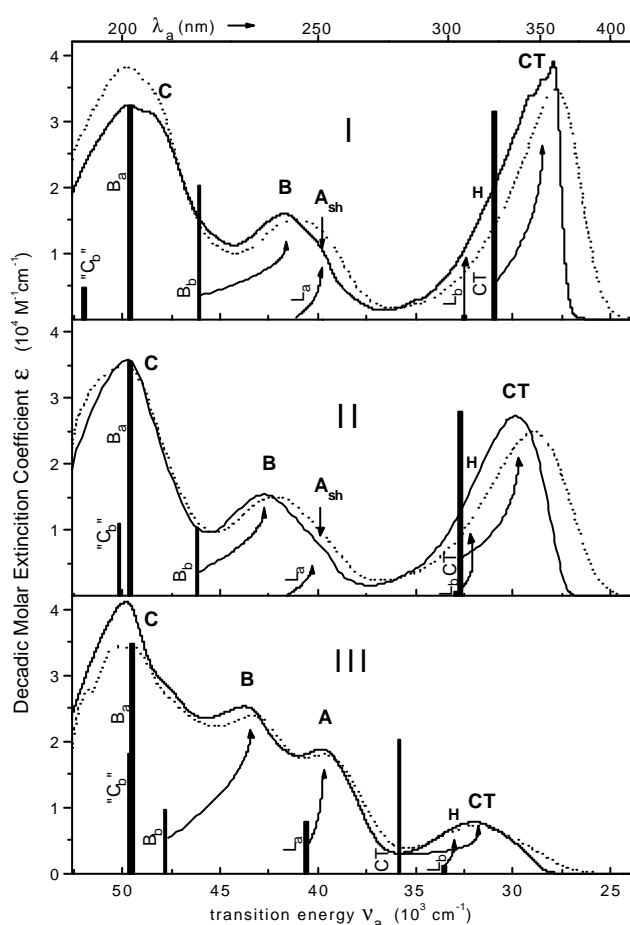


Fig. 2.2 Absorption spectra of **I-III** in n-hexane (—) and acetonitrile (---). Band notations are taken from SUZUKI.<sup>18,33</sup> The column bars symbolize the calculated transitions (gas phase) for **II** at 0°, 39° and 70°. The energy positions of the calculated transition bars are shifted by 1700 cm<sup>-1</sup> to the red and the molar extinction coefficients  $\epsilon$  are calculated from the oscillator strength for a Gaussian intensity distribution with a half width of 3400 cm<sup>-1</sup>. The arrows indicate the proposed assignments.

strongest bands by 4000 cm<sup>-1</sup>.<sup>10</sup> Besides, for each of the <sup>1</sup>L<sub>b</sub> and <sup>1</sup>L<sub>a</sub> combinations the energies have been averaged (compare transition energy differences in Fig. 2.1b) and the corresponding oscillator strengths have been summed up.

Following increasing transition energy, the empirical band labels H, A, B, C have been introduced for **BP** absorption spectra in the literature.<sup>18,34,37</sup> Within PLATT's nomenclature and the symmetry corrections based on improved calculations including configuration interaction by HAM and RUEDEBERG,<sup>38</sup> the short-axis polarized H (hidden) and B bands in **BP** can be assigned to <sup>1</sup>L<sub>b</sub> and <sup>1</sup>B<sub>b</sub> benzenoid transitions and the long-axis polarized A and C bands belong to the corresponding <sup>1</sup>L<sub>a</sub> and <sup>1</sup>B<sub>a</sub> type transitions, respectively. Let us now localize these band series in the absorption spectra of **I-III** in n-hexane (Fig.2.2).